Damage evolutions in sinter powder metals

S. Ma, M. Schneider, H. Yuan*

University of Wuppertal, Department of Mech. Engineering, Germany

* Email: h.yuan@uni-wuppertal.de

Keywords: Sintered metal, micromechanical model, damage evolution, machining effects

Abstract. The sintered powder metals have found extensive engineering applications in automobile industry. Mechanical property of sintered metals is characterized by high porosity and micro-cracks in powder metals. Inelastic behavior of the materials is coupled with micro-crack propagation and coalescence of open voids. In the present paper the damage evolution of sintered iron is determined by tension and torsion test. The tests indicated that damage of sintered iron initiated as soon as material is plastified. The damage process of sintered iron can be divided into three stages: the primary stage with high growth rate, secondary stage with stable growth rate and fracture where the growth rate is too large to measure. Fracture occurs without significant side necking. The machining of sintered metal has significant influence on the material behavior of sintered metal.

1. Introduction

Sintered metals have found extensive applications in most different areas. One important advantage of this technology is high utilization rate of material up to 95% [11], so additional mechanical treatments in many sintered parts are not required. The manufacturing process of sintered metals is a nearly net-shape process. Powder metallurgy (PM) technology has many advantages in comparison with melting metallurgy technology, e.g. low manufacturing cost, high production efficiency and flexible composition of metal elements. With development of powder metallurgy technology many high performance components working under high and complex loading conditions are of PM steel in recent years. One may expect more loading mechanical parts will also be manufactured from sintered metals [9]. For these reasons, research has focused to understand the damage mechanisms und inelastic deformations of sintered metals recently. Mechanical property of sintered metals is characterized by high porosity and micro-cracks in matrix. Inelastic behavior of the material is coupled with micro-crack propagation and coalescence of voids. The remaining pores/voids after sintering in metals reduce strength and ductility of the material. Under monotonic tensile loading condition the porosity reduces the effective load bearing cross-sectional area and acts as a stress-concentration site for damage. In particular, the fraction, size, distribution and morphology of the porosity affect on mechanical properties of sintered steel. With an increase in porosity fraction (>5%) the porosity tends to be inter-connected as a pores-net, whereas pores are relatively isolated with a small porosity fraction (<5%). Interconnected porosity causes an increase in the localization of strain at relatively smaller sintered regions between particles, while isolated porosity results in more homogeneous deformation [2,7,8].

Microscopic damage mechanism of sintered steel is investigated in monotonic in-situ tensile tests [1]. It is found that micro-cracks always initiate at pores of which the long axis is perpendicular to the tensile axis. These micro-cracks open and/or propagate in the mode I crack direction. Danninger et al. [4] measured effective loading section areas from SEM observations of the fracture surfaces of specimens broken in fatigue or impact tests and found fracture occurred with negligible plastic deformations. The damage variable is defined based on the effective loading section areas and related to Young's modulus [4]. Straffelini et al. [3] studied evolution of damage in sintered iron

by monitoring both Young's modulus and density changes during tensile testing and argued that damage is developed in two stages: the first stage contains plastic deformations limited to pore edges, and the second stage the bulk deformations becomes dominant [3]. Chawla and Deng [2] used stress controlled tests to assess the fatigue damage of sintered steel in uniaxial tension-compression cases and monitor changes of Young's modulus during loading cycles. It is shown that the damage developed quickly in the early stage of fatigue life under relative high loading [2]. All these observations have not be built in a theoretical frame.

In the present work, we are using the damage concept to describe degradation of sintered iron. The damage evolution of material is investigated under both tension and torsion loading conditions. The damage variable is determined by monitoring the change of Young's modulus or shear modulus during tension and torsion tests. Both MPA-specimen and thin-walled tube specimen were fabricated using pure iron powder ASC.100.29. The MPA-specimen was used as reference specimen to study the machining effect on mechanical properties of sintered iron.

2. Materials and experimental procedure

The pure iron powder (atomized Hoeganaes ASC.100.29) from Hoeganaes Corporation was used to produce the specimens. The organic binder (0.6% HDL-wax) is added into iron powder to improve lubricity during compaction of green parts. Basic mechanical property of the material is tested from the MPA specimen (Fig. 1). The MPA-tensile specimen is fabricated directly by compaction und sintering process. Additionally, the density of specimen was determined by Archimedes method and image analysis.

For producing tubular specimen, iron powders were compacted into cylindrical blanks with a diameter of 200mm and sintered at 1120°C for 60 min in the 95% N_2-5% H_2 atmosphere. The density of material after sintering was 7.2g/cm^3. The binder was burned out in the first stage of sintering. All tubular specimens shown in Fig. 2 were machined from the blanks. From each cylindrical blank 6 tubular specimens were fabricated. The average density of specimens after machining was increased to 7.4 g/cm^3, which is higher than the density after sintering, so the machining effect on the mechanical properties should be investigated by comparing with the MPA-tensile specimen without machining. The MPA tensile specimen has the same density and sintering condition as thin-walled tube specimen in its initial state.

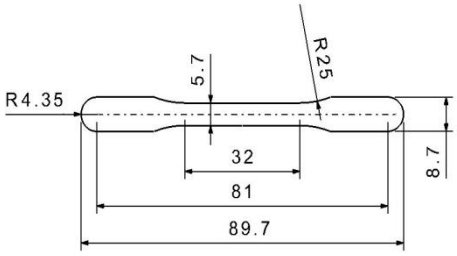

Figure 1. MPA specimen without machining

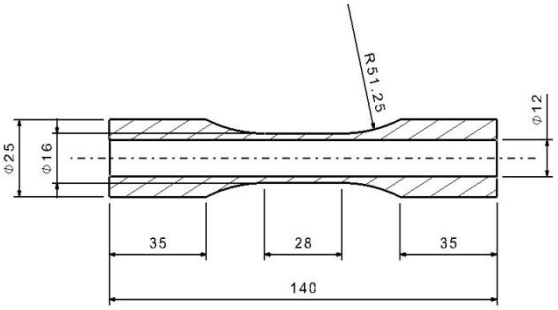

Figure 2. Thin-walled tube specimen by machining

All tests were performed at a strain rate 10^{-4}/s and at room temperature in MTS 809 axial/torsion testing machine. The gauge length of the extensometer used was 25mm. The torsion tests were performed with the tubular specimen, which has only small stress gradient and smooth stress distribution in the torsion test. The tensile tests were carried out with both MPA-tensile specimen and tubular specimen for investigating machining effect. Several loading-unloading cycles were carried out to determine the evolution of Young's modulus or shear modulus during plastic deformation. In each cycle, the loading was strain-controlled and unloading was controlled by the

stress. Young's modulus or shear modulus was determined in the unloading phase according to the Lemaitre's suggestion [10].

3. Experimental results

3.1 Microstructure characterization

The porosity of tubular specimens was measured before and after machining by image analysis technique, respectively. Optical micrographs revealed a significant decrease of porosity after machining. The porosity of specimen before machining was 8.5%. After machining of tube specimen, the porosity reduced to 6%. In other words, the material of specimen was densified from 7.2g/cm^3 to 7.4g/cm^3 after machining.

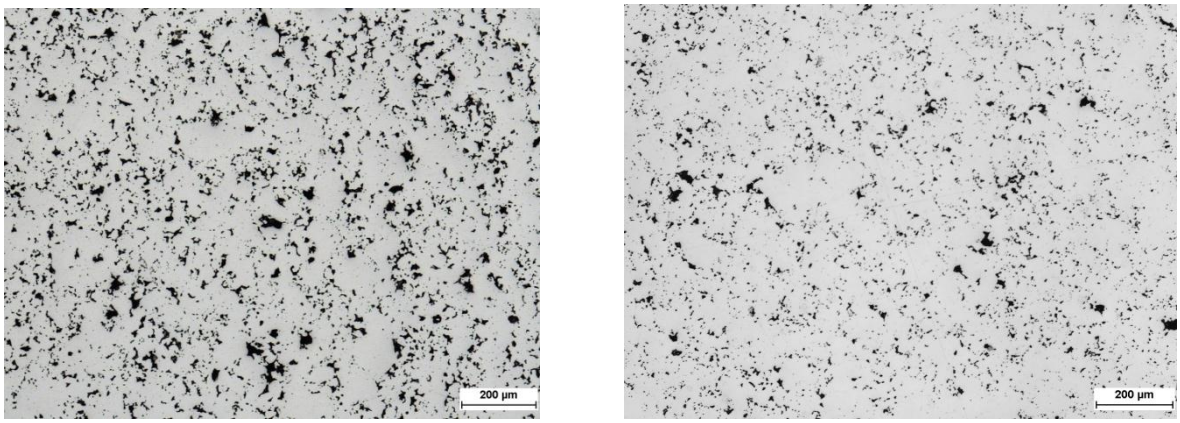

(a) (b)

Figure 3. Microstructures of the sintered iron ASC.100.29 with density 7.2g/cm^3. (a) Before machining. (b) The material is densified by machining. The density increases to 7.4g/cm^3.

3.2 Machining effects on mechanical properties

For investigating the effect of machining on mechanical properties of sintered iron, tensile tests were carried out with both MPA und tubular specimens. The MPA tensile specimen, which is the standard specimen for tension test of sintered steel according to DIN EN ISO 2740, is as-sintered without additional machining. In Fig.4, it is shown that the as-sintered MPA specimen shows a distinct Lüder's band, whereas it cannot be observed in the tubular specimen. The Lüder's band seems to disappear after machining.

More mechanical properties of both as-sintered and machined specimens are summarized in Table 1. Young's modulus of the tubular specimen significantly increases duo to densification during machining. According to the approach of Ramakrishnan and Arunachala, the R-A model, Young's modulus is expressed as a function of the porosity of material as

$$E = E_0 \left[\frac{(1 - p)^2}{1 + k_E p} \right], \qquad (1)$$

where p is the porosity of material, E_0 is the Young's modulus of fully dense material (according to literature the Young's modulus of fully dense iron is 201 GPa) [3], and κ_E is a constant in terms of Poisson's ratio of the fully dense material, ν_0,

$$k_E = 2 - 3\nu_0. \qquad (2)$$

Poisson's ratio of iron is approximately 0.3. Using R-A model, Young's modulus of specimen is 150GPa for the density 7.2 g/cm^3 and 166GPa for the density 7.4 g/cm^3. The prediction agrees with experiments of the sintered iron. However, yield stress and tensile strength seem not sensitive to the machining. The most dramatic change is observed in the fracture strain, whereas the MPA specimen

shows 12.3%, the machined specimen is broken at 4.2% elongation. This could be as a result of damage in the machining process.

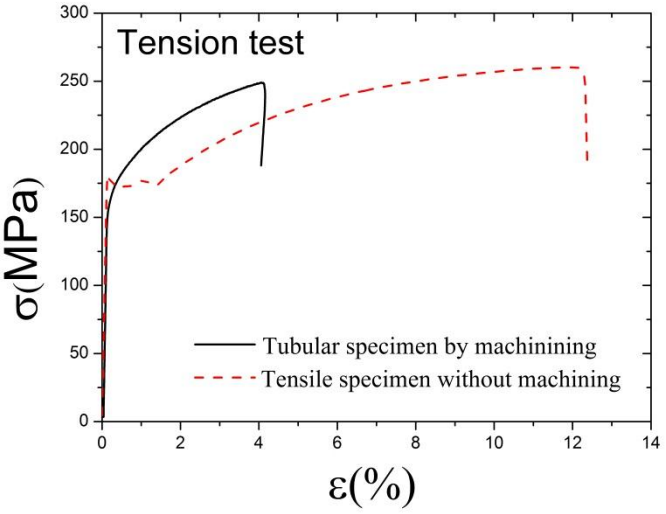

Figure 4. Tensile tests of different specimens

Table 1. Comparison of mechanical properties between MPA specimen and tubular specimen.

Specimen Type	Density [g/cm^3]	E [GPa]	σ_y [MPa]	σ_u [MPa]	ε_f [%]
MPA specimen without machining	7.2	143	135	255	12.3
Tubular specimen after machining	7.4	163	130	248	4.2

Summarizing the observations above, one may conclude that the machining on sintered iron will harden and embrittle material significantly. Effects of machining are substantial for sintered metals. It implies that mechanical property determined in MPA specimens is not related to the machined parts, especially for failure prediction.

3.3 Damage evolution

The damage evolution of sintered iron in tension and torsion test is determined by monitoring the changes of Young's modulus or shear modulus. Several loading and unloading steps were performed to trace development of damage as shown in Fig. 5. According to the effective stress concept, the damage indicator is related with Young's modulus or shear modulus as

$$D = 1 - \frac{E}{E_0} \text{ or } D = 1 - \frac{G}{G_0}, \tag{3}$$

where E_0 and G_0 are Young's modulus and shear modulus of undamaged material, respectively. The damage evolution is shown in Fig. 6, where the damage indicator was plotted as a function of the equivalent plastic strain. It is well known that the damage of material is coupled with plastic deformation. Using the J_2 plasticity theory, the equivalent plastic strain in tension-torsion test is defined as

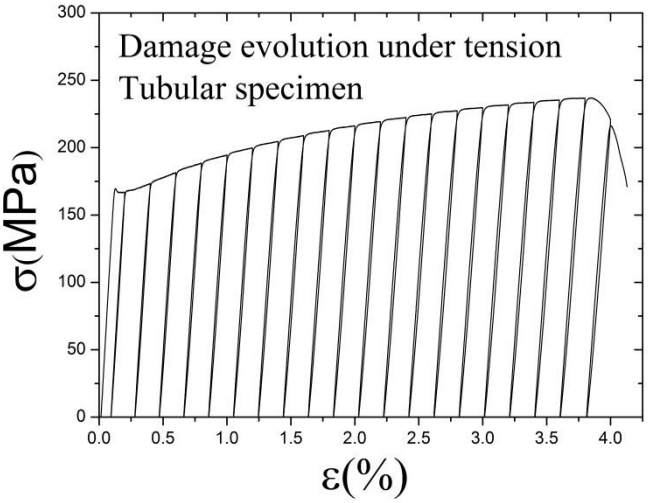

Figure 5. Loading-unloading cycles for determining damage evolution in tension test

$$e_p^{eq} = \sqrt{e_p^2 + \frac{g_p^{\ 2}}{3}}\ , \tag{4}$$

where ε_p is tensile plastic strain, and γ_p torsional plastic strain. In plastic deformations Poisson ratio is assumed to be 0.5.

Figure 6 shows results for both MPA and tubular specimens were used to investigate evolution of material damage defined in (3). All curves display convex variations, which do not agree with the damage evolution in most dense metals. It means that the sintered metal is damaged already in very low loading levels. The damage increases rapidly with the plasticization of material, then grows into a stable phase, and finally failure. That is, sintered metal damage consists of three stages: the primary stage, the secondary stage and final fracture.

- In the primary stage damage initiated as soon as material is macroscopically plastic. Due to weak links between metal particles from sintering, many connections between particles fail or micro-cracks grow into the connections. At the same time many new micro-cracks initiate. Macroscopic elasticity modulus decreases rapidly with plastic deformation. The damage increases dramatically in this stage.
- In the secondary stage, the weakest links are broken and micro-cracks grow into zones with higher fracture toughness. Macroscopic elasticity modulus becomes stable, and the damage growth rate became relatively slow.
- The final fracture stage is reached as the average stress/strain of whole tensile/torsional specimen exceeds a critical level. The specimen fails suddenly since the sintered metal is an almost brittle material.

Effects of machining are obvious in the damage evolution, as shown in Fig. 6. Damage progresses in the machined specimen more quickly than that in MPA specimens. This phenomenon is related with the densification and cold work from machining. Dramatic difference in fracture strains indicates machining-induced damage in the tubular specimen.

The experiments reveal, furthermore, that the damage evolution under shearing is very similar to that under tension under calibration of the equivalent plastic strain. But the fracture strain of torsion is dramatically larger than that from tension, which could imply correlation with the stress triaxiality in sintered iron. Generally, with higher stress triaxiality one may expect more brittle fracture.

The critical damage value is an important parameter for damage mechanics. In the sintered metals, the growth rate of the damage near the critical value is very small. It depends on machining

status. The as-sintered metal show much higher critical damage value than that of the machined specimens, whereas the shear specimen fails almost at the same critical damage as the tension. Due to brittle fracture behavior the failure is not accompanied by significant plastic deformations.

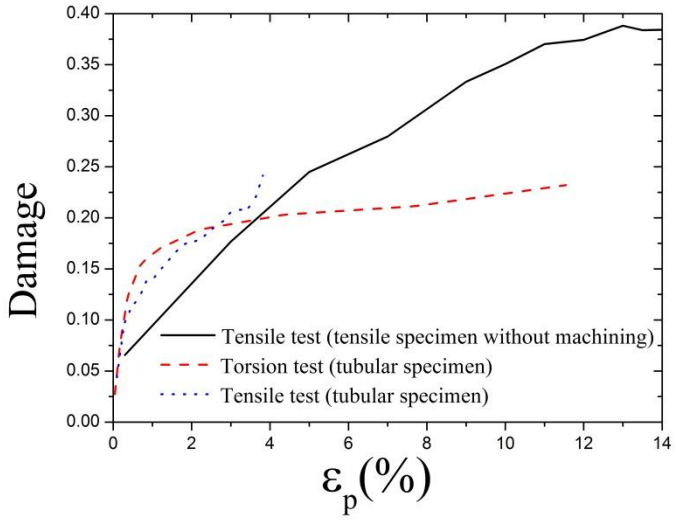

Figure 6. Damage evolution for three different specimens

4. Conclusion

Machining effect on the mechanical properties of specimen has been investigated in the present paper. Damage evolution in sintered metals was investigated experimentally, in both tension and torsion tests. The following conclusions can be made:

- Machining of sintered iron specimen has significant influence on the mechanical properties of the sintered iron. During machining the material is densified and hardened. Young's modulus increases due to densification of material. Fracture strain decreases in comparison with as-sintered specimen.
- The damage process in sintered metals can be divided in primary stage, secondary stage and fracture. Damage of sintered iron initiates as soon as plastification occurs, due to the presence of irregular pores in the microstructure, which act as stress concentration and damage initiation sites.
- Fracture strain in torsion test is much larger than in tension test. The hydrostatic stress influenced damage evolution of sintered iron. The critical damage parameter for both tension and torsion test is nearly same.

References

[1] Carabajar, S., Verdu, C., & Fougeres, R. (1997, July). Damage mechanisms of a nickel alloyed sintered steel during tensile tests. *Materials Science and Engineering: A*.

[2] Chawla, N., & Deng, X. (2005). Microstructure and mechanical behavior of porous sintered steels. *Materials Science and Engineering: A*, *390*(1-2), 98-112.

[3] Straffelini, G., & Molinari, a. (2002). Evolution of tensile damage in porous iron. *Materials Science and Engineering: A*, *334*(1-2), 96-103.

[4] H. Danninger, D. Spoljaric, B. Weiss, J. Preitfellner, *Adv. Powder Metall*. Part. Mater. 5 (1992) 227.

[5] Candela, N., Velasco, F., & Torralba, J. M. (1999). Fracture mechanisms in sintered steels with 3.5%(wt.) Mo. *Materials Science and Engineering: A*, *259*(1), 98-104.
[6] Chawla, N., Jester, B., & Vonk, D. T. (2003). Bauschinger effect in porous sintered steels. *Materials Science and Engineering: A*, *346*(1-2), 266-272.
[7] Schneider.M, Yuan.H (2010). Experimental and computational analysis of damage evolution in porous sintered irons of miniature specimens. Proceedings of 42nd. National Conference on Fracture Process, German Society of Materials Testing, Paderborn, Feb. 2010.
[8] Schneider.M, Yuan.H. Experimental und computational investigation of cyclic behavior of sintered iron. *Computational Material Science* 57(2012) 48-58
[9] Sonsino, C. M. Zukunftsperspektiven für die Pulvermetallurgie durch die Betriebsfestigkeit. *Materialwissenschaft und Werkstofftechnik*, 37(3), 240-248.
[10] J. Lemaitre. A Course on Damage Mechanics. Springer Verlag, Berlin,1987
[11] W.Schatt, K.P. Wieters, B.Kieback. Pulvermetallurgie, Springer Verlag, Berlin, 2007
[12] ABAQUS Theory Manual Version 6.10. Simulia Inc., 2009